CH_3 Rotational Tunnelling in Alkali Acetates and Correlation between NMR Spin-Lattice Relaxation and Neutron Scattering Data

A.-S. Montjoie and W. Müller-Warmuth

Institut für Physikalische Chemie der Westfälischen Wilhelms-Universität, Münster

Z. Naturforsch. **40a**, 596–601 (1985); received April 12, 1985

NMR spin-lattice relaxation rates $1/T_1$ have been measured at 15 and 30 MHz and various temperatures in polycristalline sodium and potassium acetate. The results for CH_3COONa are characteristic of methyl group tunnelling with a frequency which is very much larger than the NMR Larmor frequency. Derived values of the torsion energy (1.1 kJ/mol) and the ground state tunnel splitting (5.6 μeV) agree with data obtained from inelastic neutron scattering by Clough et al. The shape of the hindering potential and the activation energy for classical reorientation (3.2 kJ/mol) have been determined. Since the relaxation rate of CH_3COOK is a superposition of at least two mechanisms, in this case the results are less accurate and refer to one type of CH_3 rotor only: activation energy 5.4 kJ/mol, tunnel splitting 0.23 μeV. Comparison is made between tunnel splittings and classical activation energies for the acetates and various other materials: strong correlations are demonstrated and discussed.

1. Introduction

Rotational tunnelling of methyl groups at low temperatures has generated much interest since it provides the simplest example of molecular motion in solids. It is an ideal model for other motions and has been studied both in the quantum mechanical regime and as thermally activated random motion at higher temperatures. Information concerning CH_3 rotation has been obtained first of all from nuclear magnetic resonance (NMR) spectroscopy and inelastic neutron scattering (INS). Various materials have been examined: Large tunnel splittings have been observed in methyl benzenes [1–9], methyl pyridines [10–13], methyl metal compounds [14–18], acetates [7, 19–23], and a few other molecular crystals [7, 9, 24–29].

At low temperatures, tunnelling manifests itself as a splitting of the torsional ground state. If this splitting is larger than about 0.3 μeV it can be directly observed by inelastic neutron scattering [4, 5, 11, 13, 16–18, 20, 21, 23, 24, 26, 27]. Smaller tunnel splittings can be determined most effectively by using field-cycling NMR spectroscopy [6, 8, 9, 25, 28, 29]. Furthermore, if proton spin-lattice relaxation rates $1/T_1$ are measured and plotted against reciprocal temperatures, in general more than one maximum occurs, and from this and other deviations from the classical relaxation behaviour information about tunnelling can be obtained [1–4, 10, 12, 13, 14, 16–18, 19, 22, 30]. Toward higher temperature, there is a transition from quantum tunnelling to thermally activated CH_3 rotation which can be studied by both NMR relaxation and quasi-elastic neutron scattering.

It is the purpose of the present study to compare NMR and INS data of the various materials and to present further spin-lattice relaxation measurements. In this connection we have been particularly interested in correlations between the parameters associated with methyl tunnelling at low temperatures and classical reorientation at high temperatures. Among other things, neutron scattering has been extensively investigated in several acetates [20, 21, 23], but with the exception of CH_3COOLi [19], there is a need for nuclear magnetic resonance measurements of alkali acetates. This seemed to be the more important since it was claimed that relaxation rates are frequency-independent [22], which was hardly believable.

2. Experimental Details and Results

Sodium and potassium acetate were purchased from the Merck company and carefully dried by

---

Reprint requests to Professor Dr. W. Müller-Warmuth, Institut für Physikalische Chemie der Westfälischen Wilhelms-Universität, Schloßplatz 4–7, 4400 Münster.

0340-4811 / 85 / 0600-0596 $ 01.30/0. – Please order a reprint rather than making your own copy.

standard procedures. Oxygen was removed by several freeze-pump-thaw cycles, and the samples were then sealed in glass ampoules.

The NMR experiments were carried out using a Bruker SXP pulsed spectrometer at Larmor frequencies of $\omega_0/2\pi = 15$ and 30 MHz. $90° - \tau - 90°$ pulse sequences were applied, and $1/T_1$ was determined from the initial slope of the plot $\ln \frac{M_0 - M_z}{M_0}$ vs. time. According to the model of "symmetry restricted spin diffusion" [31, 32] non-exponential relaxation recovery was observed in CH_3COONa, while the relaxation in CH_3COOK was exponential. In order to control the temperature between 15 K and 110 K, home-made probes were inserted into a continous flow liquid helium cryostat from Oxford Instruments. The temperature was measured by a Ni-Cr/Au-0.02 at% Fe thermocouple. The accuracy was better than about ± 0.5 K.

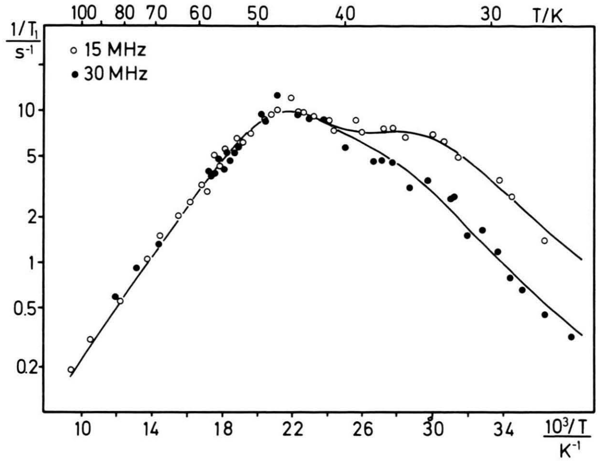

Fig. 1. Experimental proton spin-lattice relaxation rates for sodium acetate plotted against reciprocal temperatures (points). The solid lines correspond to the theoretical description using (1) and (2).

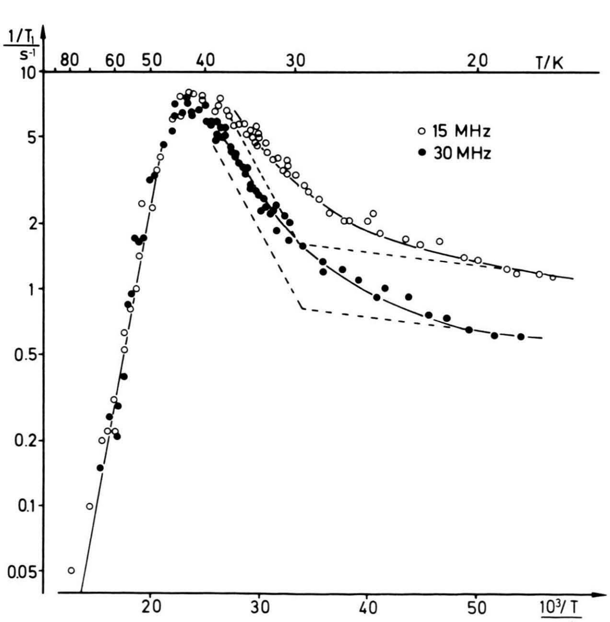

Fig. 2. Experimental proton spin-lattice relaxation rates for potassium acetate plotted against reciprocal temperatures (points). The solid lines correspond to the evaluation at low and high temperatures as discussed in the text.

Figures 1 and 2 show the experimental spin-lattice relaxation rates (points) plotted against reciprocal temperatures. Both curves are asymmetric as to be expected for tunnelling frequencies which are larger than the Larmor frequency. For sodium acetate the behaviour is reminiscent of that from many previous measurements [2–4, 13], while for potassium acetate the two maxima usually observed are not distinguishable. Unusual is in addition the decay of $1/T_1$ at low temperatures, but different from what was stated in [22], there is a clear frequency-dependence.

3. Analysis of the Data and Interpretation

In the limiting case $\omega_t \gg \omega_0$ the relaxation rate is given by the expression [13, 17, 30]

$$\frac{1}{T_1} = 4 C_{AE} \frac{\tau_c}{1 + \omega_t^2 \tau_c^2} + C_{EE} \left[\frac{\tau_c}{1 + \omega_0^2 \tau_c^2} + \frac{4 \tau_c}{1 + 4 \omega_0^2 \tau_c^2} \right]. \tag{1}$$

The first term accounts for proton relaxation by magnetic dipole-dipole interaction that is connected with a rotor transition from A to E symmetry. The theoretical value of the relaxation strength $C_{AE} = 4 \cdot 10^9 \delta^2 s^{-2}$ corresponds to the intramolecular dipole interaction within a CH_3 group with an efficiency factor δ [30], which is supposed to be slightly less than one. The second term occurs as a result of those intermolecular interactions which are connected with changes between the degenerate E_a and E_b symmetry states of the methyl rotor. The value of C_{EE} depends on the importance of intermethyl interactions and therefore on the particular material.

Equation (1) was successfully applied to various systems [4, 13, 17] using the approximation

$$\frac{1}{\tau_c} = \frac{1}{\tau_0'} \exp(- E_A'/RT) + \frac{1}{\tau_0''} \exp(- E_A''/RT) \tag{2}$$

for the temperature dependence of the correlation time τ_c. The limiting E'_A and E''_A have often been identified with the activation energy E_A and the energy separation E_{01} between the torsional ground and first excited states. The tunnelling frequency ω_t depends on the temperature and is, in general, smaller than the ground state tunnel splitting ω_t^0 measured at very low temperature.

The solid lines of Fig. 1 are computer fits of (1) and (2) to the experimental points yielding the parameters of Table 1. As compared with other crystals in which CH_3 tunnelling was studied, in CH_3COONa the frequency-independent maximum of $1/T_1$ is extraordinarily high resulting in a value for C_{AE} which is larger than all known data. This can be explained only partly by the dominant intramolecular relaxation.

The value of E'_A obtained from the slope at high temperatures corresponds to the classical activation energy E_A. Within the error limits, the apparent activation energy at low temperatures E''_A is identical with the torsion energy $E_{01} = 1.0$ kJ/mol measured by INS [21].

We have used the parameters E_A and E_{01} from this study to calculate the potential hindering the CH_3 rotation. Using tabulated solutions [33] of the Schrödinger equation with the potential

$$V(\varphi) = \frac{V_3}{2}[1 + (-1)^k \cos 3\varphi] + \frac{V_6}{2}[1 + (-1)^k \cos 6\varphi], \qquad (3)$$

the three- and sixfold contributions V_3 and V_6 have been calculated. For this purpose all possible solutions V_3 and V_6 which satisfy the experimental values $E_A = 3.2$ kJ/mol and $E_{01} = 1.1$ kJ/mol are plotted in a $V_3 + V_6$ vs. $V_3/(V_3 + V_6)$ diagram (Figure 3). There are two intersections, one with $k = 0$ (no phase shift between the three- and sixfold terms) and the other one with $k = 1$ (phase shift of $\pi/2$). The solution with the larger threefold contribution ($k = 0$) is much more probable in this crystal. Thus we obtain $V_3 = 3.7$ kJ/mol and $V_6 = 0.5$ kJ/mol. Using again the numerical solutions of the Schrödinger equation this gives a ground state tunnel splitting $\hbar\,\omega_t^0 = 5.6$ µeV, in perfect agreement with the experimental value [20] of 5.7 µeV. Another way of presentation is to include the INS result into the diagram of Fig. 3 and realize that the three lines coincide in one point.

Table 1. Parameters derived from the experimental $1/T_1$-curves as explained in the text.

	CH_3COONa		CH_3COOK	
E'_A [kJ/mol]	3.2		5.4	
E''_A [kJ/mol]	1.1		(1)	1.8
			(2)	0.18
$\hbar\,\omega_t$ [µeV]	1.5	(46 K)		
C_{AE} [$10^9\,s^{-2}$]	13.6			
C_{EE} [$10^9\,s^{-2}$]	0.5			
τ'_0 [10^{-12} s]	0.11			
τ''_0 [10^{-10} s]	9.2			

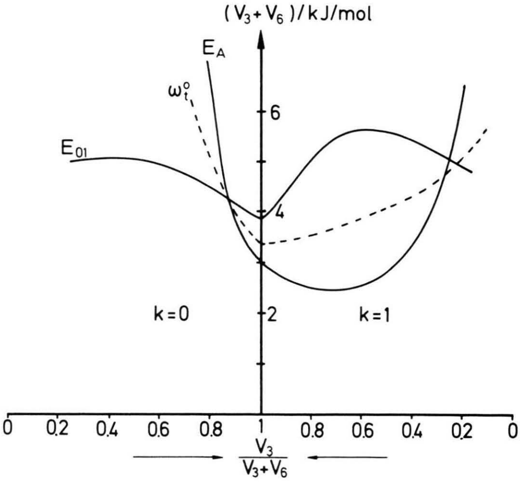

Fig. 3. Possible parameters $V_3 + V_6$ of the Schrödinger equation of the CH_3 rotor in the potential of (3) plotted against $V_3/(V_3 + V_6)$ for fixed activation and torsion energies $E_A = 3.2$ kJ/mol, $E_{01} = 1.1$ kJ/mol (solid lines). The dotted line corresponds to possible solutions for a given $\hbar\,\omega_t^0 = 5.7$ µeV.

Interpretation of the $1/T_1$ data of CH_3COOK (Fig. 2) is less clear. The missing frequency-independent maximum and the rather broad distribution near 40 K indicate that the tunnelling frequency is no longer very much larger than the NMR Larmor frequency. Both the frequency dependence of $1/T_1$ and the bending of the $10^3/T$ dependence at low temperatures can neither be explained by (1), nor by the more general relation for arbitrary values of ω_t (see, e.g., [17]). Most probably, as a consequence of the particular crystal structure, $1/T_1$ versus $10^3/T$ is a superposition of a broad and a narrow curve owing to non-equivalent methyl groups. A similar situation was discussed recently for non-equivalent methyl groups within one molecule [16, 18]. The $CH_3(1)$ rotors hindered by the larger potential barrier are more abundant and govern the central part of the curve. The very low temperature slope and perhaps the deviation near 80 K seem to belong to a second type of rotors $CH_3(2)$.

Analysis of the $1/T_1$-dependence of Fig. 2 is particularly difficult because there is in addition to the superposition the smeared and little frequency-dependent maximum, which looks similar to results that were obtained earlier in cases $\omega_t \gtrapprox \omega_0$. We have therefore confined ourselves to the evaluation of the high temperature and low temperature parts of the curve (solid lines). In such a description E'_A (see (2)) gives the activation energy $E_A(1)$, which is well defined from the measurements. The low-temperature decay of $1/T_1$, on the other hand, is decomposed into two parts (dotted lines) giving $E''_A(1)$ and $E''_A(2)$. Since such a decomposition is not free of arbitrariness, the accuracy of $E_{01}(1)$ – if identified with $E''_A(1)$ – is not very good. The numerical values are again listed in Table 1.

We have used the values of $E_A(1)$ and $E_{01}(1)$ to estimate the tunnelling frequency. Figure 4 is a similar diagram for CH_3COOK as that of Fig. 3 for CH_3COONa. From the intersection of both curves at $k = 1$ with a predominant threefold potential $V_3 = 6.2$ and $V_6 = 0.2$ kJ/mol are obtained. This would correspond to a ground state tunnel splitting of 0.23 μeV. INS measurements of the torsion and tunnel energies are in preparation in order to understand the complex behaviour of this motion completely.

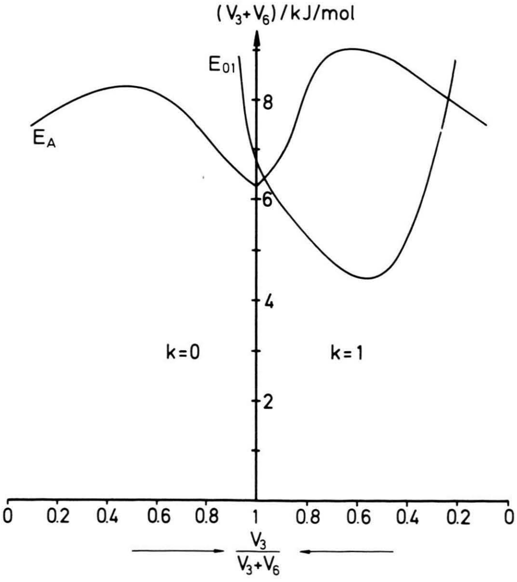

Fig. 4. Same as Fig. 3, but for activation and torsion energies $E_A = 5.4$ kJ/mol and $E_{01} = 1.8$ kJ/mol.

4. Comparison of Tunnel Splittings and Activation Energies

The results which we have obtained for the CH_3 rotation in the two acetates compare well with data known from methyl group tunnelling and rotation in other solids. In Fig. 5 we have collected the values $\hbar\,\omega_t^0$ and E_A of all materials for which both tunnel splittings and classical activation energies have been determined by INS and NMR. Only experimental values of both parameters are included. In general, tunnel splittings were measured by INS or NMR field-cycling, and activation energies by NMR-T_1.

The plot of Fig. 5 demonstrates a strong correlation between $\hbar\,\omega_t^0$ obtained at low temperatures and E_A obtained at higher temperatures. The dotted line is the tunnel splitting for a purely threefold potential plotted against the theoretical activation energy (energy difference between the top of the barrier and ground state) as derived from the solutions of the Schrödinger equation. Application of a rotational potential of the type of (3) rather than that of a purely threefold potential would result in values for $\hbar\,\omega_t^0$ either above ($k = 0$) or below ($k = 1$) the dotted line. Most of the data occur near the dotted line and this is also true for sodium acetate (j). Potassium acetate is not included, since no direct experimental value is available; but the estimated $\hbar\,\omega_t^0 = 0.23$ μeV fits well together with $E_A = 5.4$ kJ/mol.

Exceptions from the clear connection between the experimental quantum-mechanical tunnel splittings and classical activation energies occur first of all in the range of low potential barriers (a and b in Fig. 5). Here it is not at all certain that really the energy difference between the barrier and the torsional ground state is measured in a T_1-experiment. The exception e (2,6-dimethylpyridine) has been explained in the meantime. Recent INS experiments [34] revealed that there is in addition to the tunnel peak e originally measured [13] at least one more transition e′ at 38 μeV which probably belongs to

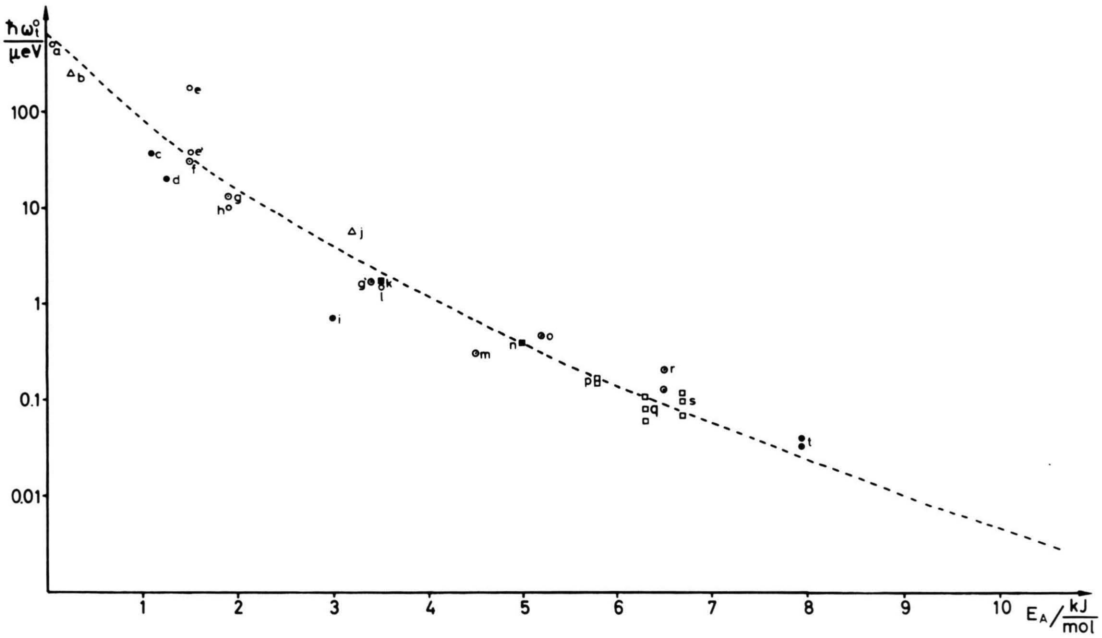

Fig. 5. $\hbar\omega_t^0$ and E_A data of various CH_3 rotors in methyl benzenes (●), methyl pyridines (○), methyl metal compounds (⊙), acetates (△) and some further materials (■, □). The experimental values are taken from the literature: a) 4-methyl-pyridine [11, 12], b) lithium acetate [19, 20], c) 4-methyl-2,6-ditertiarybutylphenol [3, 5], d) toluene [2, 4, 36], e) 2,6-dimethylpyridine [13, 35], f) tetramethyllead [18], g) tetramethyltin [16], h) 3-methylpyridine [13], i) pentamethylbenzene [1, 8], j) sodium acetate [this work], k) dimethylacetylene [24], l) 3,5-dimethylpyridine [13], m) methyllithium [17], n) acetone [28, 37], o) tetramethylgermanium [17], p) trichloromethylsilane [29], q) tetramethylpyrazine [9], r) γ-tetramethylsilane [17], s) 1,2,4,5-tetramethylbenzene [9], t) hexamethylbenzene [6].

the E_A value of 1.5 kJ/mol and which indicates the existence of non-equivalent CH_3 groups. The rather low $\hbar\omega_t^0$ value of pentamethylbenzene (i) could eventually be connected with the assignment of field-cycling data, which is not necessarily unequivocal.

Figure 5 contains measurements of different authors carried out for many years. The importance of the correlation of all these results lies in the fact that the same model can be applied for rotational tunnelling and classical reorientation over a large range of temperatures and barrier heights. When methyl group rotation is considered, it is a wrong way to distinguish between CH_3 rotors which tunnel and others which do not. The question is rather: how large is the tunnel splitting, may it be detected and how can it be observed, and what is the temperature? The continuous transition in one system between free quantum motion and thermally activated motion requires a coherent theoretical approach which is still missing [35]. For practical purposes it is possible to estimate the low temperature splitting $\hbar\omega_t^0$ from a measurement of the activation energy E_A at higher temperatures.

[1] P. S. Allen and A. Cowking, J. Chem. Phys. **49,** 789 (1968).
[2] J. Haupt and W. Müller-Warmuth, Z. Naturforsch. **23a,** 208 (1968); **24a,** 1066 (1969).
[3] S. Clough and P. A. Beckmann, J. Phys. **C 10,** L 231 (1977).
[4] W. Müller-Warmuth, R. Schüler, M. Prager, and M. Kollmar, J. Magn. Reson. **34,** 83 (1979).
[5] S. Clough and A. Heidemann, J. Phys. **C 12,** 761 (1979).
[6] S. Takeda, G. Soda, and H. Chihara, Solid State Commun. **36,** 445 (1980).
[7] S. Clough, A. Heidemann, A.-J. Horsewill, J.-D. Lewis, and M. N. J. Paley, J. Phys. **C 14,** L 525 (1981).
[8] B. Gabrys and L. van Gerven, Chem. Phys. Lett. **82,** 260 (1981).
[9] S. Takeda and H. Chihara, J. Magn. Reson. **54,** 285 (1983).
[10] J. Haupt, Z. Naturforsch. **28a,** 98 (1973).
[11] B. Alefeld, A. Kollmar, and B. A. Dasannacharya, J. Chem. Phys. **63,** 4415 (1975).
[12] A. E. Zweers, H. B. Brom, and W. J. Huiskamp, Physica **85B,** 239 (1977).

[13] W. Müller-Warmuth, R. Schüler, M. Prager, and A. Kollmar, J. Chem. Phys. **69,** 2382 (1978).
[14] D. J. Ligthelm, R. A. Wind, and J. Smidt, Physica **100 B,** 175 (1980).
[15] B. Gabrys and P. Coppens, J. Magnetism Magn. Mat. **31/34,** 747 (1983).
[16] M. Prager, K. H. Dupree, and W. Müller-Warmuth, Z. Phys. B – Condensed Matter **51,** 309 (1983).
[17] W. Müller-Warmuth, K. H. Dupree, and M. Prager, Z. Naturforsch. **37 a,** 66 (1984).
[18] M. Prager and W. Müller-Warmuth, Z. Naturforsch. **39 a,** 1187 (1984).
[19] P. S. Allen and P. Branson, J. Phys. **C 11,** L 121 (1978).
[20] S. Clough, A. Heidemann, and M. N. J. Paley, J. Phys. **C 13,** 4009 (1980).
[21] S. Clough, A. Heidemann, M. N. J. Paley, and J. B. Suck, J. Phys. **C 13,** 6599 (1980).
[22] F. Köksal, E. Rössler, and H. Sillescu, J. Phys. **C 15,** 5821 (1982).
[23] S. Clough, A. Heidemann, A. H. Horsewill, and M. N. J. Paley, Z. Phys. B – Condensed Matter **55,** 1 (1984).
[24] B. Alefeld and H. Kollmar, Phys. Lett. **A 57,** 289 (1976).
[25] P. van Hecke and G. Janssens, Phys. Rev. B **17,** 2124 (1978).
[26] J. R. Cockbain, R. Lechner, M. Owen, R. K. Thomas, and J. W. White, Mol. Phys. **45,** 1035 (1982).
[27] A. Heidemann, I. Anderson, B. Jeffryes, and B. Alefeld, Z. Phys. B – Condensed Matter **49,** 123 (1982).
[28] S. Clough, A. J. Horsewill, and P. J. McDonald, J. Phys. **C 17,** 1115 (1984).
[29] S. Takeda and H. Chihara, J. Magn. Reson. **56,** 48 (1984).
[30] J. Haupt, Z. Naturforsch. **26 a,** 1578 (1971).
[31] S. Emid and R. A. Wind, Chem. Phys. Lett. **33,** 269 (1975).
[32] S. Emid, R. J. Baarda, J. Smidt, and R. A. Wind, Physica **93 B,** 327 (1978).
[33] R. F. Gloden, Euratom Reports EUR 4349 and EUR 4358 (1970).
[34] M. Prager, private communication.
[35] S. Clough, P. J. McDonald, and F. O. Zelaya, J. Phys. **C 17,** 4413 (1984).
[36] D. Cavagnat, J. Lascombe, J. C. Lassagues, A. J. Horsewill, A. Heidemann, and J. B. Suck, J. Physique **45,** 97 (1984).
[37] D. J. Ligthelm, The Influence of the Spin-Rotor-Coupling of Methyl Groups in Solids and their NMR Relaxation, Thesis, Delft 1981.